Published in final edited form as:
Pharm Res. 2009 July ; 26(7): 1729–1738. doi:10.1007/s11095-009-9883-5.

Cellular responses to dietary cancer chemopreventive agent D,L-sulforaphane in human prostate cancer cells are initiated by mitochondrial reactive oxygen species

Dong Xiao[1,*], **Anna A. Powolny**[1,*], **Jedrzej Antosiewicz**[2], **Eun-Ryeong Hahm**[1], **Ajay Bommareddy**[1], **Yan Zeng**[3], **Dhimant Desai**[4], **Shantu Amin**[4], **Anna Herman-Antosiewicz**[5], and **Shivendra V. Singh**[1,3]

[1] Department of Pharmacology & Chemical Biology, University of Pittsburgh School of Medicine, Pittsburgh, PA [2] Department of Bioenergetics and Physiology of Exercise, Medical University of Gdansk, Gdansk, Poland [3] University of Pittsburgh Cancer Institute, Pittsburgh, PA [4] Department of Pharmacology, Penn State Milton S. Hershey Medical Center, Hershey, PA [5] Department of Molecular Biology, University of Gdansk, Gdansk, Poland

Abstract

Purpose—Present study was undertaken to elucidate the mechanism of cellular responses to D,L-sulforaphane (SFN), a highly promising cancer chemopreventive agent.

Methods—Mitochondrial DNA deficient Rho-0 variants of LNCaP and PC-3 cells were generated by culture in the presence of ethidium bromide. Apoptosis was assessed by analysis of cytoplasmic histone-associated DNA fragmentation and activation of caspase-3. Immunoblotting was performed to determine the expression of apoptosis- and cell cycle-regulating proteins. Generation of reactive oxygen species (ROS), mitochondrial membrane potential (MMP), and cell cycle distribution were measured by flow cytometry.

Results—The Rho-0 variants of LNCaP and PC-3 cells were significantly more resistant to SFN-induced ROS generation, apoptotic DNA fragmentation, disruption of MMP, cytosolic release of cytochrome *c*, and G2/M phase cell cycle arrest compared with corresponding wild-type cells. SFN-induced autophagy, which serves to protect against apoptotic cell death in PC-3 and LNCaP cells, was also partially but markedly suppressed in Rho-0 variants compared with wild-type cells. SFN statistically significant inhibited activities of mitochondrial respiratory chain enzymes in LNCaP and PC-3 cells.

Conclusion—These results indicate, for the first time, that mitochondria-derived ROS serve to initiate diverse cellular responses to SFN exposure in human prostate cancer cells.

Keywords

Sulforaphane; Prostate Cancer; Chemoprevention

Requests for reprints: Shivendra V. Singh, 2.32A Hillman Cancer Center Research Pavilion, 5117 Centre Avenue, Pittsburgh, PA 15213. Phone: 412-623-3263; Fax: 412-623-7828. Email: singhs@upmc.edu.
*Equal contribution.

Introduction

Epidemiological data continues to lend support to the idea that dietary intake of cruciferous vegetables may lower the risk of different types of malignancies including cancer of the prostate (1–4). Anticarcinogenic effect of cruciferous vegetables is attributed to organic isothiocyanates (ITCs), which are released upon processing (cutting and chewing) of these vegetables due to myrosinase-mediated hydrolysis of corresponding glucosinolates (5,6). Broccoli is a rather rich source of the ITC compound (−)-1-isothiocyanato-(4*R*)-(methylsulfinyl)-butane (L-SFN), which together with its synthetic racemic analogue D,L-sulforaphane (SFN) has received particular attention due to remarkable anticancer properties. For example, L-SFN and SFN are equipotent inducers of phase 2 drug metabolizing enzyme quinone reductase in Hepa1c1c7 murine hepatoma cells (7). Exposure of prostate cancer cells to L-SFN resulted in transcriptional up-regulation of γ-glutamylcysteine synthetase light subunit and glutathione transferases (8). The L-SFN or synthetic SFN has been shown to afford significant protection against 9,10-dimethyl-1,2-benzanthracene-induced mammary carcinogenesis in rats, azoxymethane-induced colonic aberrant crypt foci in rats, and benzo[*a*]pyrene-induced forestomach cancer in mice (9–11). Dietary feeding of SFN inhibited malignant progression of lung adenomas induced by tobacco carcinogens in A/J mice (12).

More recent studies including those from our laboratory have documented novel cellular responses to SFN exposure in cultured human cancer cells, including G2/M phase cell cycle arrest, induction of apoptosis and autophagy, inhibition of histone deacetylase, protein binding, and sensitization of cells to TRAIL-induced apoptosis (13–25). The SFN-mediated signal transduction pathways culminating into growth arrest and apoptosis induction have been extensively studied in human prostate cancer cells (15–17,19–21,25). For example, we have shown previously that the SFN-induced apoptosis is selective towards prostate cancer cells and correlates with generation of reactive oxygen species (ROS) (18,19). The SFN-induced apoptosis in prostate cancer cells was accompanied by depletion of intracellular glutathione levels and blunted by antioxidants (19). Pretreatment of prostate cancer cells with antioxidants including *N*-acetylcysteine and a combined mimetic of superoxide dismutase and catalase (EUK134) as well as adenovirus-mediated transduction of catalase conferred significant protection against SFN-induced ROS generation, apoptotic DNA fragmentation, cytosolic release of cytochrome *c*, collapse of mitochondrial membrane potential, and caspase activation (19). These results pointed towards critical role of ROS in signal transduction by SFN (19). We have also shown previously that oral gavage of SFN significantly retards growth of PC-3 human prostate cancer xenografts in nude mice and inhibits prostate carcinogenesis and pulmonary metastasis in a transgenic mouse model of prostate cancer (26,27).

Despite these advances, however, the mechanism by which SFN causes ROS production remains elusive. In the present study we generated mitochondrial DNA deficient Rho-0 variants of LNCaP and PC-3 cells to determine possible involvement of mitochondria in anticancer signal transduction by SFN. We now demonstrate, for the first time, that cellular responses to SFN exposure (cell cycle arrest, apoptosis induction and autophagy) in human prostate cancer cells are initiated by the mitochondria-derived ROS due to inhibition of mitochondrial respiratory chain (MRC) enzymes.

Materials and Methods

Reagents

SFN (purity >99%) was synthesized as described by Conaway et al. (12). SFN was stored at −20°C and found to be stable for at least four months as judged by high-performance liquid chromatography (12). Reagents for cell culture including F-12K Nutrient Mixture, RPMI 1640 medium, penicillin and streptomycin antibiotic mixture, and serum were purchased from

GIBCO (Grand Island, NY). Hydroethidine (HE), 6-carboxy-2′,7′-dichlorodihydrofluorescein diacetate (H_2DCFDA), and 5,5′,6,6′-tetrachloro-1,1′,3,3′-tetraethylbenzimidazolocarbocyanine iodide (JC-1) were purchased from Molecular Probes (Eugene, OR) whereas 4′,6-diamidino-2-phenylindole (DAPI) was obtained from Sigma (St. Louis, MO). The ELISA kit for quantitation of cytoplasmic histone-associated DNA fragmentation was from Roche Diagnostics (Mannheim, Germany). The antibody against cytochrome *c* oxidase subunit IV (COXIV) was from Molecular Probes; the anti-cytochrome *c* antibody was from BD Pharmingen (Palo Alto, CA); antibodies against Bax, Bak, cyclinB1, Tyr15 phosphorylated cyclin-dependent kinase 1 (cdk1), and Ser10 phosphorylated histone H3 were from Santa Cruz Biotechnology (Santa Cruz, CA); anti-catalase antibody was from Calbiochem (Gibbstown, NJ); antibody against microtubule-associated protein 1 light chain 3 (LC3) was from Cell Signaling (Danvers, MA); and anti-Bcl-2 antibody was from DAKO Cytomation (Carpinteria, CA).

Cell Lines and Generation of Rho-0 Variants

Monolayer cultures of PC-3 cells were maintained in F-12K Nutrient Mixture supplemented with 7% non-heat inactivated fetal bovine serum and antibiotics. The LNCaP cells were cultured in RPMI 1640 supplemented with 10% fetal bovine serum, 2.4 mg/mL glucose, 1 mmol/L sodium pyruvate, and antibiotics. Both cell lines were maintained at 37°C in an atmosphere of 5% CO_2 and 95% air. The Rho-0 variants of LNCaP and PC-3 cells were generated and maintained as described previously by King and Attadi (28) with some modifications. Briefly, the cells were cultured in complete medium supplemented with 1 mmol/L sodium pyruvate, 1 mmol/L uridine and 2.5 μmol/L ethidium bromide over a period of seven weeks. Cells cultured in parallel in medium without ethidium bromide were used as controls (wild-type cells).

Immunocytochemical Analysis for COXIV

Wild-type and Rho-0 variants of LNCaP and PC-3 cells (1×10^5) were plated on coverslips and allowed to attach by overnight incubation. Cells were first treated with 200 nmol/L MitoTracker Red at 37°C for 30 min to stain mitochondria. After washing with PBS, the cells were fixed with 2% paraformaldehyde overnight at 4°C and permeabilized using 0.1% Triton X-100 in PBS for 10 min. The cells were washed with PBS, blocked with 0.5% bovine serum albumin (BSA) in PBS for 1 h, and incubated with anti-COXIV antibody overnight at 4°C. The cells were then washed with PBS, incubated with Alexa Fluor 488-conjugated secondary antibody (1:1000 dilution, Molecular Probes) for 1 h at room temperature. Subsequently, the cells were washed with PBS and treated with DAPI (10 ng/mL) for 5 min at room temperature to stain nuclear DNA. The cells were washed twice with PBS and examined under a Leica fluorescence microscope at 40× objective lens magnification.

Immunoblotting

The cells were treated with 20 μmol/L SFN for 24 h and lysed as described by us previously (29). The mitochondria-free cytosolic fraction for immunoblotting of cytochrome *c* was prepared as described by us previously (25). The lysate proteins were resolved by 6–12.5% sodium dodecyl sulfate polyacrylamide gel electrophoresis and transferred onto membrane. Immunoblotting was performed as described by us previously (21,25,29).

Measurement of MRC Enzyme Activities

Cells were plated at a density of 1×10^6 in 100-mm culture dishes, allowed to attach by overnight incubation, and treated with DMSO (control) or different concentrations of SFN for 6 h at 37°C. Cells were then harvested by scraping, washed with PBS, and lysed. Protein concentration was determined using the Bradford reagent. Activity of complex I-linked NADH-ubiquinone

oxidoreductase, complex II-linked succinate-ubiquinone oxidoreductase, and complex III-linked ubiquinol cytochrome *c* reductase was determined as described by us previously (30).

Measurement of ROS Generation

Intracellular ROS generation in DMSO-treated control and SFN-treated cells (20 μmol/L SFN for 4 h) was measured by flow cytometry following staining with HE and H_2DCFDA as described by us previously (19). The 2′,7′-dichlorofluorescein (DCF) fluorescence was measured using a Coulter Epics XL Flow Cytometer.

Determination of Apoptotic DNA Fragmentation, Cell Viability, and Caspase-3 Activation

Apoptosis induction by SFN was assessed by analysis of cytoplasmic histone-associated DNA fragmentation using a kit from Roche Diagnostics according to the manufacturer's instructions. Activation of caspase-3 was determined by flow cytometry using a kit from Cell Signaling. The cells were treated with DMSO (control) or SFN for specified time period, and processed for flow cytometric analysis of caspase-3 activation according to the manufacturer's instructions. The effect of SFN treatment on cell viability was determined by trypan blue dye exclusion assay as described by us previously (31).

Measurement of Mitochondrial Membrane Potential (MMP) and Cell Cycle Distribution

MMP was measured using a potential-sensitive dye JC-1 (32). Stock solution of JC-1 (1 mg/mL) was prepared in DMSO and freshly diluted with the assay buffer. Briefly, cells (2×10^5) were plated in T25 flasks, allowed to attach by overnight incubation, exposed to desired concentrations of SFN for specified time periods, and collected by trypsinization. The cells were incubated with medium containing JC-1 (10 μg/mL) for 15 min at 37°C. The cells were washed, re-suspended in 0.5 mL assay buffer, and analyzed using a Coulter Epics XL Flow Cytometer. Mitochondrial uncoupler carbonylcyanide 4-(trifluoromethoxy)phenylhydrazone (FCCP; 25 μM) was used as a positive control. The effect of SFN treatment on cell cycle distribution was determined by flow cytometry following staining the cells with propidium iodide essentially as described by us previously (15). Cells in different phases of the cell cycle were computed for DMSO-treated control and SFN-treated cultures.

Detection of Autophagy

Autophagy induction by SFN was assessed by (a) analysis of acidic vesicular organelles by fluorescence microscopy following staining with lysosomotropic agent acridine orange, (b) immunoblotting for cleavage of LC3, and (c) immunofluorescence microscopy to determine recruitment of LC3 to autophagosomes essentially as described by us previously (21).

Statistical Analysis

One-way ANOVA followed by Bonferroni's multiple comparison test or t-test was used to determine statistical significance of difference in measured variables between control and treated groups. Difference was considered significant at $P<0.05$.

Results

Rho-0 Variants of LNCaP and PC-3 Cells were Resistant to ROS Generation and Apoptosis Induction by SFN

To determine role of mitochondria in ROS generation by SFN, we generated Rho-0 variants of LNCaP and PC-3 cells by culture in the presence of ethidium bromide. The survival of Rho-0 cells is dependent on ATP derived from anaerobic glycolysis but these cells have functional F1-ATPase (33–35). The Rho-0 cells are unable to generate ROS from MRC. Initially, we carried out experiments to confirm Rho-0 phenotype of the variant LNCaP and PC-3 cells. As

can be seen in Fig. 1A, the mitochondria in wild-type cells were brightly stained with MitoTracker red and COXIV, which is encoded by the mitochondrial DNA, as revealed by fluorescence microscopy. The intensity of the MitoTracker red and COXIV staining was much weaker in Rho-0 cells than in the wild-type cells (Fig. 1A). Consistent with these results, immunoblotting revealed expression of COXIV in wild-type LNCaP and PC-3 cells but not in their Rho-0 variants (Fig. 1B). In addition, the Rho-0 variants of LNCaP and PC-3 cells exhibited significantly diminished activities of complex I (Fig. 1C) and complex III (Fig. 1D) of the MRC. These results confirmed Rho-0 phenotype of the variant LNCaP and PC-3 cells.

Next, we proceeded to determine the effect of SFN treatment on ROS generation and apoptosis induction using wild-type LNCaP and PC-3 cells and their Rho-0 variants. As expected, exposure of wild-type LNCaP and PC-3 cells to 20 μmol/L SFN for 4 h resulted in ROS generation as evidenced by a statistically significant increase in DCF fluorescence over DMSO-treated control (Fig. 2A). The SFN-mediated increase in DCF fluorescence was not observed in the Rho-0 variants of LNCaP and PC-3 cells (Fig. 2A). The SFN treatment (20 μmol/L, 24 h) caused significant increase in cytoplasmic histone-associated DNA fragmentation in the wild-type LNCaP and PC-3 cells compared with corresponding DMSO-treated controls (Fig. 2B). The SFN-mediated cytoplasmic histone-associated DNA fragmentation was significantly lower in Rho-0 variants of LNCaP and PC-3 cells compared with corresponding wild-type cells (Fig. 2B). The Rho-0 cells were significantly more resistant to SFN-mediated suppression of cell viability compared with the wild-type cells (Fig. 2C). These results clearly indicated that SFN-mediated apoptosis induction and growth inhibition in both LNCaP and PC-3 cells are initiated by the mitochondria-derived ROS.

ROS Acted Upstream of Caspase-3 Activation and MMP Collapse in SFN-induced Apoptosis

Next, we determined the effect of SFN treatment on caspase-3 activation, MMP, and cytochrome *c* release using wild-type PC-3 cells and its Rho-0 variant. Twenty-four hour exposure of wild-type PC-3 cells to 20 μmol/L SFN resulted in about 10-fold enrichment of active caspase-3 (Fig. 3A). The SFN-mediated activation of caspase-3 was only 2-fold higher over DMSO-treated control in Rho-0 variant of PC-3 cells (Fig. 3A). Next, we determined effect of SFN treatment on MMP using JC-1 dye. The collapse of the MMP is characterized by green fluorescence due to accumulation of monomeric JC-1 in the cytosol (32). The SFN treatment (20 μmol/L, 4 h) caused a marked increase in monomeric JC-1-associated green fluorescence in wild-type PC-3 cells, which was nearly completely inhibited in the Rho-0 variant (Fig. 3B). Treatment with 20 μmol/L SFN for 24 h resulted in cytosolic release of cytochrome *c* in wild-type PC-3 cells but not in its Rho-0 variant (Fig. 3C). Collectively, these results indicated that ROS acted upstream of disruption of MMP and caspase-3 activation in SFN-induced apoptosis.

SFN-mediated Changes in Levels of Bcl-2 Family Proteins

We addressed the question of whether resistance of Rho-0 cells to SFN-mediated apoptosis was due to lack of change in ratio of proapoptotic to anti-apoptotic Bcl-2 family protein levels. As can be seen in Fig. 3C, SFN treatment (20 μmol/L, 24 h) caused marked induction of Bax protein level and modest decline in the levels of Bcl-2 protein in wild-type PC-3 cells. These changes were not apparent in the Rho-0 variant of PC-3 cells (Fig. 3C). Interestingly, the stress caused by depletion of mitochondrial DNA in Rho-0 PC-3 variant also resulted in up-regulation of both Bax and Bcl-2, but not Bak, in comparison with wild-type cells (Fig. 3C). These results provided further evidence that mitochondria-derived ROS acted upstream of Bax induction in regulation of SFN-induced apoptotic cell death.

Critical Role of ROS in SFN-induced G2/M Phase Cell Cycle Arrest

We designed experiments to test a hypothesis that the initial signal for SFN-mediated G2/M phase cell cycle arrest stems from ROS production. As can be seen in Fig. 4A, twenty-four hour exposure of wild-type LNCaP cells to 20 μmol/L SFN resulted in enrichment of G2/M fraction over DMSO-treated control. The SFN-mediated G2/M phase cell cycle arrest was not evident in the Rho-0 variant of LNCaP cells (Fig. 4A). Likewise, the Rho-0 variant of PC-3 cells was significantly more resistant to SFN-mediated G2/M phase cell cycle arrest compared with wild-type PC-3 cells (results not shown). We performed immunoblotting for key proteins involved in regulation of G2/M transition to confirm resistance of Rho-0 cells towards SFN-induced cell cycle arrest. As shown in Fig. 4B, the SFN treatment (20 μmol/L, 24 h) resulted in upregulation of cyclinB1 and increased Tyr15 phosphorylation (inactivation) of cdk1 in wild-type PC-3 cells, which was not observed in the Rho-0 variant (Fig. 4B). The SFN treatment also increased Ser10 phosphorylation (a marker of mitotic cells) of histone H3 in wild-type PC-3 cells but not in its Rho-0 variant (Fig. 4B). The immunoblotting for cell cycle regulatory proteins also suggested that Rho-0 cells were probably growth arrested in G2 and mitotic phases as evidenced by increased phosphorylations of cdk1 and histone H3, respectively, in DMSO-treated Rho-0 PC-3 cells (Fig. 4B). Collectively, these results indicated that (a) the mitochondrial stress resulting from depletion of mitochondrial DNA caused growth arrest even in the absence of SFN treatment, and (b) the signal transduction for SFN-induced G2/M phase cell cycle arrest was also initiated by the mitochondria-derived ROS.

SFN-induced Autophagy Was Partially Inhibited in Rho-0 Cells

Autophagy induction is another novel cellular response to SFN exposure in cultured prostate cancer cells and serves to protect against apoptotic cell death caused by SFN treatment (21). A very recent study has implicated ROS and catalase degradation in autophagy regulation (36). We therefore raised the question of whether autophagic response to SFN in prostate cancer cells was also linked to ROS generation. As shown in Fig. 5A, SFN treatment had minimal effect on catalase protein level in wild-type LNCaP and PC-3 cells as well as in their Rho-0 variants. We determined autophagic response to SFN in wild-type LNCaP and PC-3 cells and their Rho-0 variants by analysis of processing and recruitment of LC3 and formation of AVOs, which are hallmarks of autophagy (37–41). The LC3 protein (18 kDa) is cleaved by autophagic stimuli to a 16 kDa intermediate (LC3-II) that localizes to the autophagosomes (37). As can be seen in Fig. 5A, SFN treatment resulted in cleavage of LC3 in both wild-type LNCaP and PC-3 cells. The SFN-mediated cleavage of LC3 was partially but markedly suppressed in Rho-0 variants of both cell lines (Fig. 5A). Recruitment of LC3-II to the autophagosomes is characterized by punctate pattern of its localization (21,37,38). The DMSO-treated (9 h exposure) wild-type PC-3 (Fig. 5B) and LNCaP cells (results not shown) exhibited diffuse and weak LC3-associated green fluorescence. On the other hand, the wild-type PC-3 cells (Fig. 5B) and LNCaP cells (results not shown) treated for 9 h with 40 μmol/L SFN exhibited punctate pattern of LC3 immunostaining. The SFN-induced recruitment of LC3 to autophagosomes was much less pronounced in the Rho-0 variants of PC-3 (Fig. 5C) and LNCaP cells (results not shown). In agreement with these results, the SFN-induced (40 μmol/L, 9 h) formation of AVOs was relatively more pronounced in the wild-type PC-3 (Fig. 5D) and LNCaP cells (results not shown) than in their Rho-0 variants. The SFN-mediated recruitment of LC3 to autophagosomes in PC-3 cells stably transfected with plasmid encoding GFP-LC3 (21) was also significantly inhibited by pre-treatment with *N*-acetylcysteine (supplemental Fig. S1). Collectively these results indicated that SFN-induced autophagy was partially dependent on ROS production.

SFN Treatment Inhibited Activities of MRC

To identify the target of SFN-mediated ROS generation, we determined its effect on activities of MRC enzymes using LNCaP and PC-3 cells. SFN treatment (6 h) resulted in significant

inhibition of complex-I, II, and III activities in both LNCaP (Fig. 6A) and PC-3 cell lines especially at 40–100 μmol/L SFN (Fig. 6B). However, complex II was most sensitive to inhibition by SFN in both cell lines at 40–100 μmol/L concentrations. Nonetheless, these results indicated that SFN treatment caused inhibition of MRC leading to ROS generation in human prostate cancer cells.

Discussion

Even though possible contribution of ROS in apoptotic response to the ITC family of cancer chemopreventive agents, including phenethyl-ITC, was suggested previously (42,43), the mechanism of ROS generation by this class of chemopreventive agent was not clear. The present study indicates that ROS production in SFN-treated prostate cancer cells is mitochondria-derived. The mitochondrial DNA deficient Rho-0 variants of LNCaP and PC-3 cells are significantly more resistant to ROS generation, growth suppression, and apoptosis induction by SFN compared with wild-type cells. Moreover, SFN treatment causes significant inhibition of MRC complex activities in both LNCaP and PC-3 cells. While further studies are needed to determine the precise mechanism of SFN-mediated inhibition of MRC enzymes, it is plausible that SFN covalently modifies critical subunit(s) of MRC complexes. This possibility is meritorious because ITC/SFN-mediated covalent modification of cellular proteins has been documented previously (24,44).

ROS function upstream of cytochrome *c* release and caspase activation by certain apoptotic stimuli such as hyperoxia (45). At the same time, generation of ROS downstream of the release of cytochrome *c* has also been described in some cellular models of mitochondria-mediated apoptosis (46,47). The present study reveals that ROS act upstream of mitochondrial changes in SFN-induced apoptosis because collapse of MMP and cytosolic release of cytochrome *c* are observed in wild-type cells but not in Rho-0 variants. Consistent with these results, the Rho-0 variant of PC-3 cell line is also resistant to SFN-mediated activation of caspase-3. Previous studies have shown that SFN-induced apoptosis correlates with induction of multidomain proapoptotic proteins Bax and Bak and down-regulation of anti-apoptotic protein Bcl-2 (18, 19,25,26). We found that SFN-mediated induction of Bax, but not Bcl-2 down-regulation, is also dependent on ROS generation.

The present study shows that the G2/M phase cell cycle arrest caused by SFN exposure is initiated by mitochondria-derived ROS. The SFN-mediated G2/M phase cell cycle arrest is observed in wild-type LNCaP cells but not in its Rho-0 variant. The Rho-0 variant of PC-3 cell line is also significantly more resistant to SFN-induced G2/M phase cell cycle arrest compared with wild-type cells (results not shown). Eukaryotic cell cycle progression involves sequential activation of cdks whose activation is dependent upon their association with regulatory cyclins (48). A complex formed by the association of cdk1 (also known as $p34^{cdc2}$) with cyclinB1 plays a major role in regulation of G2/M transition (48). Activity of cdk1/cyclinB1 kinase complex is negatively regulated by reversible phosphorylations at Thr14 and Tyr15 of cdk1 (48). The SFN-mediated inhibition of G2/M progression in wild-type prostate cancer cells is associated with an increase in Tyr15 phosphorylation of cdk1 suggesting inhibition of the cdk1/cyclinB1 kinase complex. Because SFN treatment causes an increase in protein level of cyclinB1 in wild-type cells, it is reasonable to conclude that the cell cycle arrest in our model is unlikely to be due to inhibition of complex formation between cdk1 and cyclinB1. Our data also suggest that the Rho-0 cells with mitochondrial stress exhibit growth arrest even in the absence of SFN treatment as evidenced by hyperphosphorylation of cdk1 at Tyr15 and accumulation of mitotic marker Ser-10 phosphorylated histone H3.

Recent studies have implicated ROS in autophagic response to various stimuli including chemical inhibitors of MRC and caspase inhibitor zVAD (36,49). For example, autophagic

cell death resulting from treatment of murine L929 cell line with caspase inhibitor zVAD was shown to be associated with ROS generation and degradation of catalase (36). Interestingly, the ROS generation and catalase degradation occurred down-stream of zVAD-mediated autophagy in L929 cells (36). In contrast, the results of the present study indicate that SFN-mediated autophagy, which serves to protect against SFN-induced apoptosis at least in LNCaP and PC-3 cells (21), is partially dependent upon ROS. The SFN-mediated autophagy is relatively more pronounced in the wild-type LNCaP and PC-3 cells compared with their Rho-0 variants as judged by analysis of LC3 cleavage and recruitment and formation of AVOs. Thus, we conclude that ROS serve to partially contribute to autophagy induction by SFN in prostate cancer cells.

In conclusion the present study offers a mechanistic model for cellular response to SFN in human prostate cancer cells involving ROS, which are mitochondria-derived and serve to function upstream of apoptosis, G2/M phase cell cycle arrest, and autophagy. The translational implication of these findings is that cancer chemopreventive effect of SFN may be attenuated in the presence of anti-oxidants.

Supplementary Material

Refer to Web version on PubMed Central for supplementary material.

Acknowledgments

Grant support: This investigation was supported in part by the USPHS grants CA115498 and CA101753 (to S.V.S.), awarded by the National Cancer Institute, and grant 2718/P01/2007/32 (to A.H-A.), awarded by the Polish Ministry of Science and Higher Education.

References

1. Verhoeven DT, Goldbohm RA, van Poppel G, Verhagen H, van den Brandt PA. Epidemiological studies on *Brassica* vegetables and cancer risk. Cancer Epidemiol Biomarkers Prev 1996;5:733–748. [PubMed: 8877066]
2. Kolonel LN, Hankin JH, Whittemore AS, Wu AH, Gallagher RP, Wilkens LR, John EM, Howe GR, Dreon DM, West DW, Paffenbarger RS Jr. Vegetables, fruits, legumes and prostate cancer: a multiethnic case-control study. Cancer Epidemiol Biomarkers Prev 2000;9:795–804. [PubMed: 10952096]
3. Zhang SM, Hunter DJ, Rosner BA, Giovannucci EL, Colditz GA, Speizer FE, Willett WC. Intakes of fruits, vegetables, and related nutrients and the risk of non-Hodgkin's lymphoma among women. Cancer Epidemiol Biomarkers Prev 2000;9:477–485. [PubMed: 10815692]
4. Ambrosone CB, McCann SE, Freudenheim JL, Marshall JR, Zhang Y, Shields PG. Breast cancer risk in premenopausal women is inversely associated with consumption of broccoli, a source of isothiocyanates, but is not modified by GST genotype. J Nutr 2004;134:1134–1138. [PubMed: 15113959]
5. Hecht SS. Inhibition of carcinogenesis by isothiocyanates. Drug Metab Rev 2000;32:395–411. [PubMed: 11139137]
6. Conaway CC, Yang YM, Chung FL. Isothiocyanates as cancer chemopreventive agents: their biological activities and metabolism in rodents and humans. Curr Drug Metab 2002;3:233–255. [PubMed: 12083319]
7. Zhang Y, Talalay P, Cho CG, Posner GH. A major inducer of anticarcinogenic protective enzymes from broccoli: isolation and elucidation of structure. Proc Natl Acad Sci USA 1992;89:2399–2403. [PubMed: 1549603]
8. Brooks JD, Paton VG, Vidanes G. Potent induction of phase 2 enzymes in human prostate cells by sulforaphane. Cancer Epidemiol Biomarkers Prev 2001;10:949–954. [PubMed: 11535546]

9. Zhang Y, Kensler TW, Cho CG, Posner GH, Talalay P. Anticarcinogenic activities of sulforaphane and structurally related synthetic norbornyl isothiocyanates. Proc Natl Acad Sci USA 1994;91:3147–3150. [PubMed: 8159717]
10. Chung FL, Conaway CC, Rao CV, Reddy BS. Chemoprevention of colonic aberrant crypt foci in Fischer rats by sulforaphane and phenethyl isothiocyanate. Carcinogenesis 2000;21:2287–2291. [PubMed: 11133820]
11. Fahey JW, Haristoy X, Dolan PM, Kensler TW, Scholtus I, Stephenson KK, Talalay P, Lozniewski A. Sulforaphane inhibits extracellular, intracellular, and antibiotic-resistant strains of *Helicobacter pylori* and prevents benzo[*a*]pyrene-induced stomach tumors. Proc Natl Acad Sci USA 2002;99:7610–7615. [PubMed: 12032331]
12. Conaway CC, Wang CX, Pittman B, Yang YM, Schwartz JE, Tian D, McIntee EJ, Hecht SS, Chung FL. Phenethyl isothiocyanate and sulforaphane and their N-acetylcysteine conjugates inhibit malignant progression of lung adenomas induced by tobacco carcinogens in A/J mice. Cancer Res 2005;65:8548–8557. [PubMed: 16166336]
13. Gamet-Payrastre L, Li P, Lumeau S, Cassar G, Dupont MA, Chevolleau S, Gasc N, Tulliez J, Tercé F. Sulforaphane, a naturally occurring isothiocyanate, induces cell cycle arrest and apoptosis in HT29 human colon cancer cells. Cancer Res 2000;60:1426–1433. [PubMed: 10728709]
14. Jackson SJT, Singletary KW. Sulforaphane: a naturally occurring mammary carcinoma mitotic inhibitor, which disrupts tubulin polymerization. Carcinogenesis 2004;25:219–227. [PubMed: 14578157]
15. Singh SV, Herman-Antosiewicz A, Singh AV, Lew KL, Srivastava SK, Kamath R, Brown KD, Zhang L, Baskaran R. Sulforaphane-induced G_2/M phase cell cycle arrest involves checkpoint kinase 2 mediated phosphorylation of Cdc25C. J Biol Chem 2004;279:25813–25822. [PubMed: 15073169]
16. Myzak MC, Hardin K, Wang R, Dashwood RH, Ho E. Sulforaphane inhibits histone deacetylase activity in BPH-1, LNCaP and PC-3 prostate epithelial cells. Carcinogenesis 2006;27:811–819. [PubMed: 16280330]
17. Cho SD, Li G, Hu H, Jiang C, Kang KS, Lee YS, Kim SH, Lu J. Involvement of c-Jun N-terminal kinase in G2/M arrest and caspase-mediated apoptosis induced by sulforaphane in DU145 prostate cancer cells. Nutr Cancer 2005;52:213–224. [PubMed: 16201852]
18. Choi S, Singh SV. Bax and Bak are required for apoptosis induction by sulforaphane, a cruciferous vegetable derived cancer chemopreventive agent. Cancer Res 2005;65:2035–2043. [PubMed: 15753404]
19. Singh SV, Srivastava SK, Choi S, Lew KL, Antosiewicz J, Xiao D, Zeng Y, Watkins SC, Johnson CS, Trump DL, Lee YJ, Xiao H, Herman-Antosiewicz A. Sulforaphane-induced cell death in human prostate cancer cells is initiated by reactive oxygen species. J Biol Chem 2005;280:19911–19924. [PubMed: 15764812]
20. Xu C, Shen G, Chen C, Gelinas C, Kong AN. Suppression of NF-kappaB and NF-kappaB-regulated gene expression by sulforaphane and PEITC through IkappaBalpha, IKK pathway in human prostate cancer PC-3 cells. Oncogene 2005;24:4486–4495. [PubMed: 15856023]
21. Herman-Antosiewicz A, Johnson DE, Singh SV. Sulforaphane causes autophagy to inhibit release of cytochrome *c* and apoptosis in human prostate cancer cells. Cancer Res 2006;66:5828–5835. [PubMed: 16740722]
22. Kim H, Kim EH, Eom YW, Kim WH, Kwon TK, Lee SJ, Choi KS. Sulforaphane sensitizes tumor necrosis factor-related apoptosis-inducing ligand (TRAIL)-resistant hepatoma cells to TRAIL-induced apoptosis through reactive oxygen species-mediated up-regulation of DR5. Cancer Res 2006;66:1740–1750. [PubMed: 16452234]
23. Pledgie-Tracy A, Sobolewski MD, Davidson NE. Sulforaphane induces cell type-specific apoptosis in human breast cancer cell lines. Mol Cancer Ther 2007;6:1013–1021. [PubMed: 17339367]
24. Mi L, Wang X, Govind S, Hood BL, Veenstra TD, Conrads TP, Saha DT, Goldman R, Chung FL. The role of protein binding in induction of apoptosis by phenethyl isothiocyanate and sulforaphane in human non-small lung cancer cells. Cancer Res 2007;67:6409–6416. [PubMed: 17616701]
25. Choi S, Lew KL, Xiao H, Herman-Antosiewicz A, Xiao D, Brown CK, Singh SV. D,L-Sulforaphane-induced cell death in human prostate cancer cells is regulated by inhibitor of apoptosis family proteins and Apaf-1. Carcinogenesis 2007;28:151–162. [PubMed: 16920735]

26. Singh AV, Xiao D, Lew KL, Dhir R, Singh SV. Sulforaphane induces caspase-mediated apoptosis in cultured PC-3 human prostate cancer cells and retards growth of PC-3 xenografts *in vivo*. Carcinogenesis 2004;25:83–90. [PubMed: 14514658]
27. Singh SV, Warin R, Xiao D, Powolny AA, Stan SD, Arlotti JA, Zeng Y, Hahm ER, Marynowski SW, Bommareddy A, Desai D, Amin S, Parise RA, Beumer JH, Chambers WH. Sulforaphane inhibits prostate carcinogenesis and pulmonary metastasis in TRAMP mice in association with increased cytotoxicity of natural killer cells. Cancer Res. 2009In Press
28. King MP, Attadi G. Mitochondria-mediated transformation of human rho(0) cells. Methods Enzymol 1996;264:313–334. [PubMed: 8965705]
29. Xiao D, Srivastava SK, Lew KL, Zeng Y, Hershberger P, Johnson CS, Trump DL, Singh SV. Allyl isothiocyanate, a constituent of cruciferous vegetables, inhibits proliferation of human prostate cancer cells by causing G_2/M arrest and inducing apoptosis. Carcinogenesis 2003;24:891–897. [PubMed: 12771033]
30. Xiao D, Powolny AA, Singh SV. Benzyl isothiocyanate targets mitochondrial respiratory chain to trigger ROS-dependent apoptosis in human breast cancer cells. J Biol Chem 2008;283:30151–30163. [PubMed: 18768478]
31. Xiao D, Choi S, Johnson DE, Vogel VG, Johnson CS, Trump DL, Lee YJ, Singh SV. Diallyl trisulfide-induced apoptosis in human prostate cancer cells involves c-Jun N-terminal kinase and extracellular-signal regulated kinase-mediated phosphorylation of Bcl-2. Oncogene 2004;23:5594–5606. [PubMed: 15184882]
32. Cossarizza A, Baccarani-Contri M, Kalashnikova G, Franceschi C. A new method for the cytofluorimetric analysis of mitochondrial membrane potentials using the J-aggregate forming lipophilic cation 5, 5′, 6, 6′-tetrachloro-1, 1′, 3, 3′-tetraethylbenzimidazolylcarbocyanine iodide (JC-1). Biochem Biophys Res Commun 1993;197:40–45. [PubMed: 8250945]
33. Buchet K, Godinot C. Functional F1-ATPase essential in maintaining growth and membrane potential of human mitochondrial-DNA depleted ρ° cells. J Biol Chem 1998;273:22983–22989. [PubMed: 9722521]
34. Chandel NS, Schumacker PT. Cells depleted of mitochondrial DNA (rho0) yield insight into physiological mechanisms. FEBS Lett 1999;454:173–176. [PubMed: 10431801]
35. Chandel NS, McClintock DS, Feliciano CE, Wood TM, Melendez JA, Rodriguez AM, Schumacker PT. Reactive oxygen species generated at mitochondrial complex III stabilize hypoxia-inducible factor 1 α during hypoxia: a mechanism of O_2 sensing. J Biol Chem 2000;275:25130–25138. [PubMed: 10833514]
36. Yu L, Wan F, Dutta S, Welsh S, Liu Z, Freubndt E, Baehrecke EH, Lenardo M. Autophagic programmed cell death by selective catalase degradation. Proc Natl Acad Sci USA 2006;103:4952–4957. [PubMed: 16547133]
37. Kabeya Y, Mizushima N, Ueno T, Yamamoto A, Kirisako T, Noda T, Kominami E, Ohsumi Y, Yoshimori T. LC3, a mammalian homologue of yeast Apg8p, is localized in autophagosome membranes after processing. EMBO J 2000;21:5720–5728. [PubMed: 11060023]
38. Paglin S, Hollister T, Delohery T, Hackett N, McMahill M, Sphicas E, Domingo D, Yahalom J. A novel response of cancer cells to radiation involves autophagy and formation of acidic vesicles. Cancer Res 2001;61:439–444. [PubMed: 11212227]
39. Kanzawa T, Kondo Y, Ito H, Kondo S, Germano. Induction of autophagic cell death in malignant glioma cells by arsenic trioxide. Cancer Res 2003;63:2103–2108. [PubMed: 12727826]
40. Daido S, Kanzawa T, Yamamoto A, Takeuchi H, Kondo Y, Kondo S. Pivotal role of the cell death factor BNIP3 in ceramide-induced autophagic cell death in malignant glioma cells. Cancer Res 2004;64:4286–4293. [PubMed: 15205343]
41. Kanzawa T, Germano IM, Komata T, Ito H, Kondo Y, Kondo S. Role of autophagy in temozolomide-induced cytotoxicity for malignant glioma cells. Cell Death Differ 2004;11:448–457. [PubMed: 14713959]
42. Xiao D, Lew KL, Zeng Y, Xiao H, Marynowski SM, Dhir R, Singh SV. Phenethyl isothiocyanate-induced apoptosis in PC-3 human prostate cancer cells is mediated by reactive oxygen species-dependent disruption of the mitochondrial membrane potential. Carcinogenesis 2006;27:2223–2234. [PubMed: 16774948]

43. Trachootham D, Zhou Y, Zhang H, Demizu Y, Chen Z, Pelicano H, Chiao PJ, Achanta G, Arlinghaus RB, Liu J, Huang P. Selective killing of oncogenically transformed cells through a ROS-mediated mechanism by B-phenylethyl isothiocyanate. Cancer Cell 2006;10:241–252. [PubMed: 16959615]
44. Mi L, Wang X, Govind S, Hood BL, Veenstra TD, Conrads TP, Saha DT, Goldman R, Chung FL. The role of protein binding in induction of apoptosis by phenethyl isothiocyanate and sulforaphane in human non-small lung cancer cells. Cancer Res 2007;67:6409–6416. [PubMed: 17616701]
45. Buccellato LJ, Tso M, Akinci OI, Chandel NS, Budinger GRS. Reactive oxygen species are required for hyperoxia-induced Bax activation and cell death in alveolar epithelial cells. J Biol Chem 2004;279:6753–6760. [PubMed: 14625274]
46. Gottlieb E, Vander Heiden MG, Thompson CB. Bcl-x(L) prevents the initial decrease in mitochondrial membrane potential and subsequent reactive oxygen species production during tumor necrosis factor alpha-induced apoptosis. Mol Cell Biol 2000;20:5680–5689. [PubMed: 10891504]
47. Cai J, Jones DP. Superoxide in apoptosis. Mitochondrial generation triggered by cytochrome *c* loss. J Biol Chem 1998;273:11401–11404. [PubMed: 9565547]
48. Hartwell LH, Kastan MB. Cell cycle control and cancer. Science 1994;266:1821–1828. [PubMed: 7997877]
49. Chen Y, McMillan-Ward E, Kong J, Israels SJ, Gibson SB. Mitochondrial electron-transport-chain inhibitors of complexes I and II induce autophagic cell death mediated by reactive oxygen species. J Cell Sci 2007;120:4155–4166. [PubMed: 18032788]

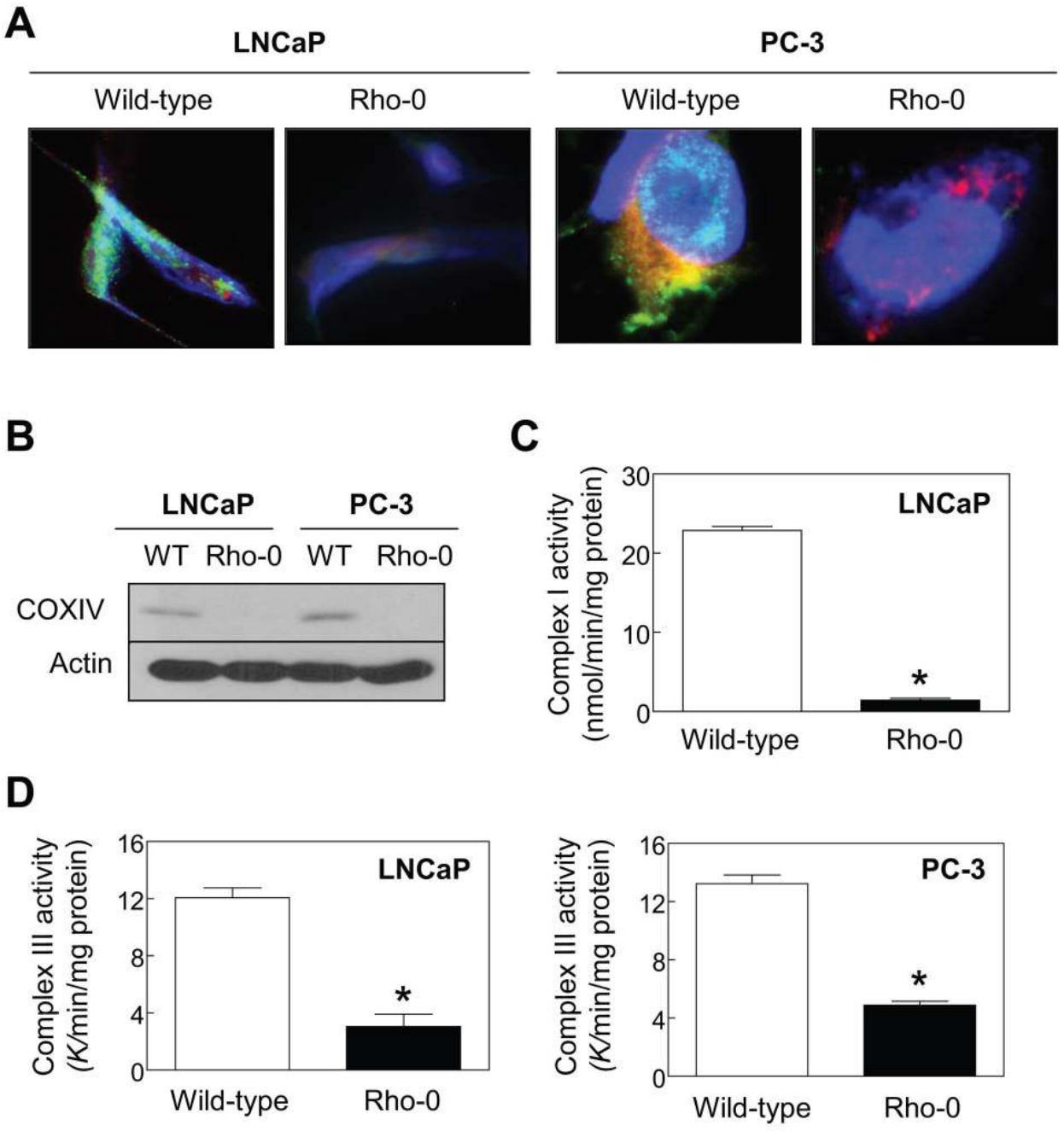

Fig. 1. Characterization of Rho-0 variants of LNCaP and PC-3 cells

A, fluorescence microscopic analysis of cytochrome *c* oxidase subunit IV (COXIV) expression in wild-type LNCaP and PC-3 cells and their Rho-0 variants. The staining for mitochondria (MitoTracker red), COXIV, and nuclei (DAPI) are indicated by *red, green* and *blue fluorescence*, respectively. **B,** immunoblotting for COXIV using lysates from wild-type LNCaP and PC-3 cells and their Rho-0 variants. **C,** activity of complex I using lysate proteins from wild-type and Rho-0 LNCaP cells. **D**, activity of complex III using lysate proteins from wild-type LNCaP and PC-3 cells and their Rho-0 variants. Results are mean ± SE of 3 determinations. *Significantly different (P<0.05) compared with wild-type cells by t-test.

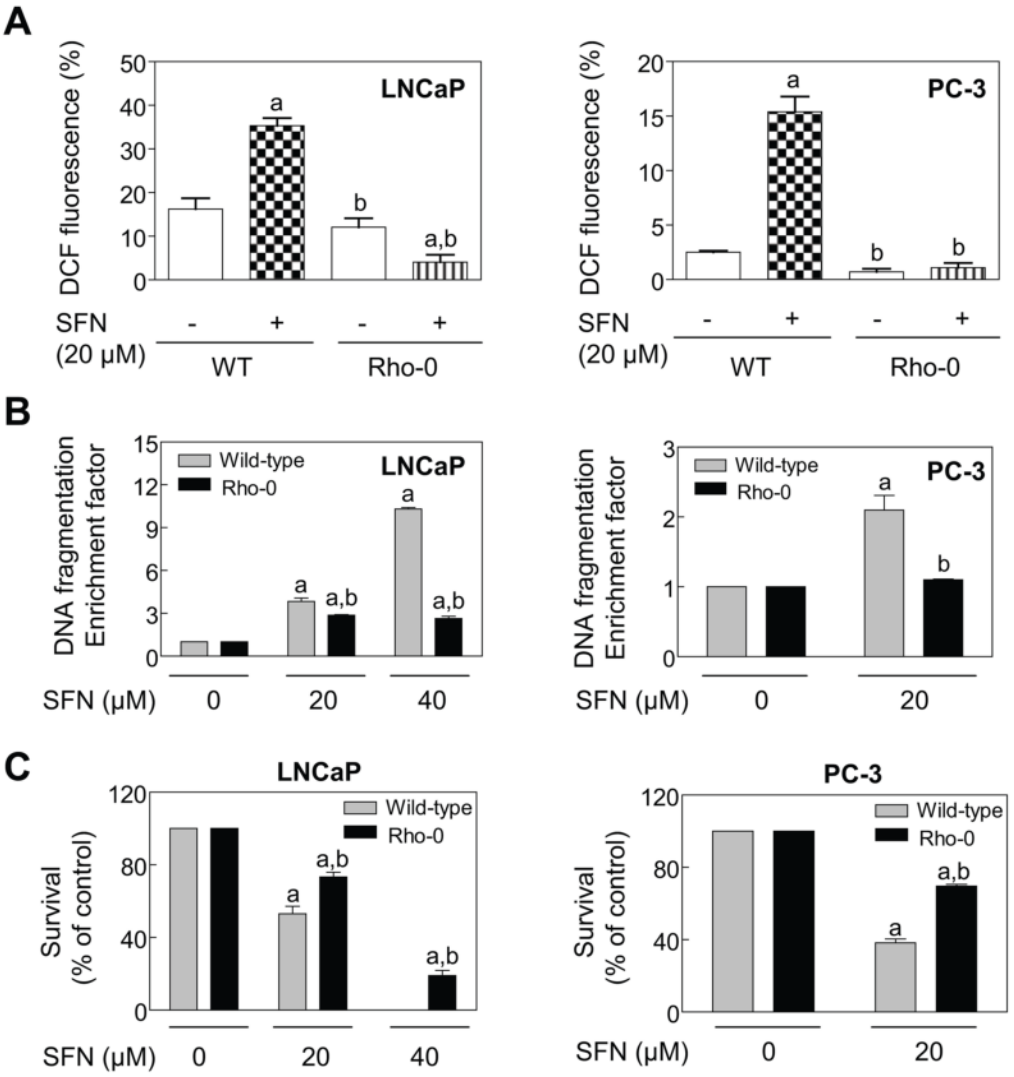

Fig. 2. Rho-0 variants of LNCaP and PC-3 cells are significantly more resistant towards ROS generation and apoptosis induction by SFN compared with wild-type cells

A, DCF fluorescence (a measure of ROS generation) in wild-type LNCaP and PC-3 cells and their Rho-0 variants following 4 h treatment with DMSO or 20 μmol/L SFN. Results are expressed as percentage of DCF positive cells. **B,** analysis of cytoplasmic histone-associated DNA fragmentation in wild-type LNCaP and PC-3 cells and their Rho-0 variants following 24 h treatment with DMSO or the indicated concentrations of SFN. Results are expressed as enrichment factor relative to DMSO-treated control for both wild-type and Rho-0 cells. **C,** trypan blue dye exclusion assay to assess cell viability in wild-type LNCaP and PC-3 cells and their Rho-0 variants following 24 h treatment with DMSO or SFN. Results are mean ± SE (n= 3). Significantly different (P<0.05) compared with [a]corresponding DMSO-treated control and [b]SFN-treated wild-type cells by one-way ANOVA followed by Bonferroni's test. Each experiment was performed at least twice with triplicate measurements in each experiment. The results were consistent and representative data from a single experiment are shown.

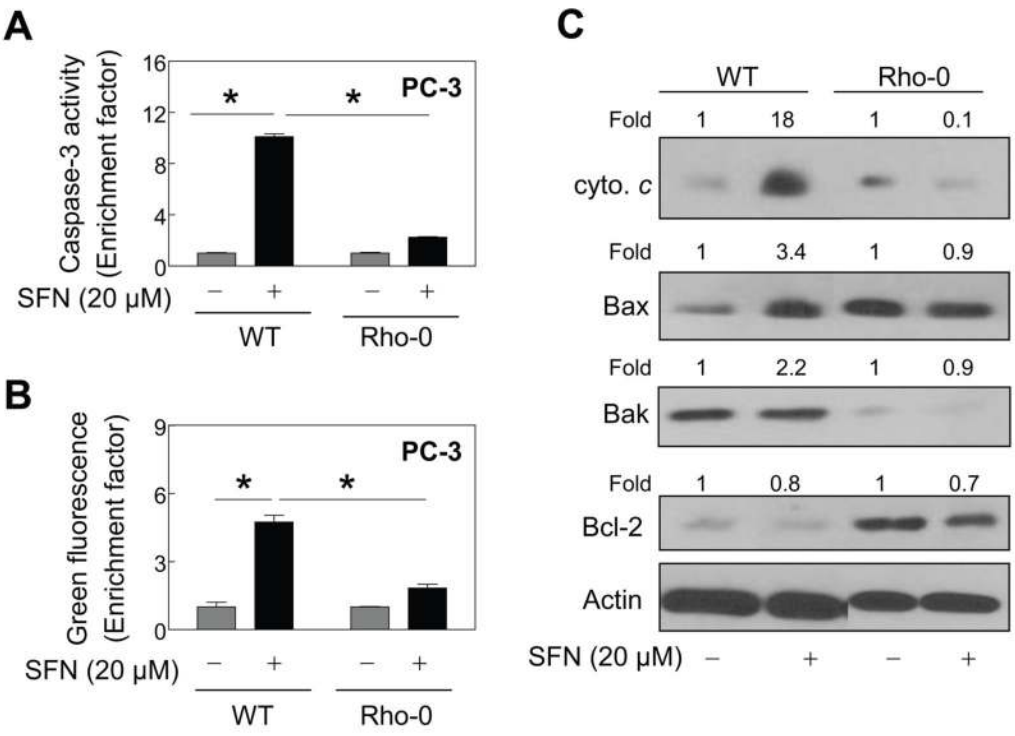

Fig. 3. ROS act upstream of mitochondrial membrane potential collapse in SFN-induced apoptosis

A, flow cytometric analysis of caspase-3 activation in wild-type PC-3 cells and its Rho-0 variant following 24 h treatment with DMSO or 20 μmol/L SFN. Results are expressed as enrichment factor relative to DMSO-treated wild-type cells. **B,** analysis of mitochondrial membrane potential collapse (monomeric JC-1-associated green fluorescence) in wild-type and Rho-0 PC-3 cells following 4 h treatment with DMSO or 20 μmol/L SFN. Results are expressed as enrichment factor relative to DMSO-treated wild-type cells. **C,** immunoblotting for cytochrome *c*, Bax, Bak, and Bcl-2 using mitochondria-free cytosolic fraction (cytochrome *c*) or whole lysates from wild-type and Rho-0 PC-3 cells treated for 24 h with DMSO or 20 μmol/L SFN. The numbers on top of the immunoreactive bands represent change in protein levels relative to DMSO-treated control in both wild-type and Rho-0 PC-3 cells. Each experiment was performed at least twice and the results were comparable. In panels A and B, results are mean ± SE (n= 3). *Significantly different (P<0.05) between the indicated groups by one-way ANOVA followed by Bonferroni's test.

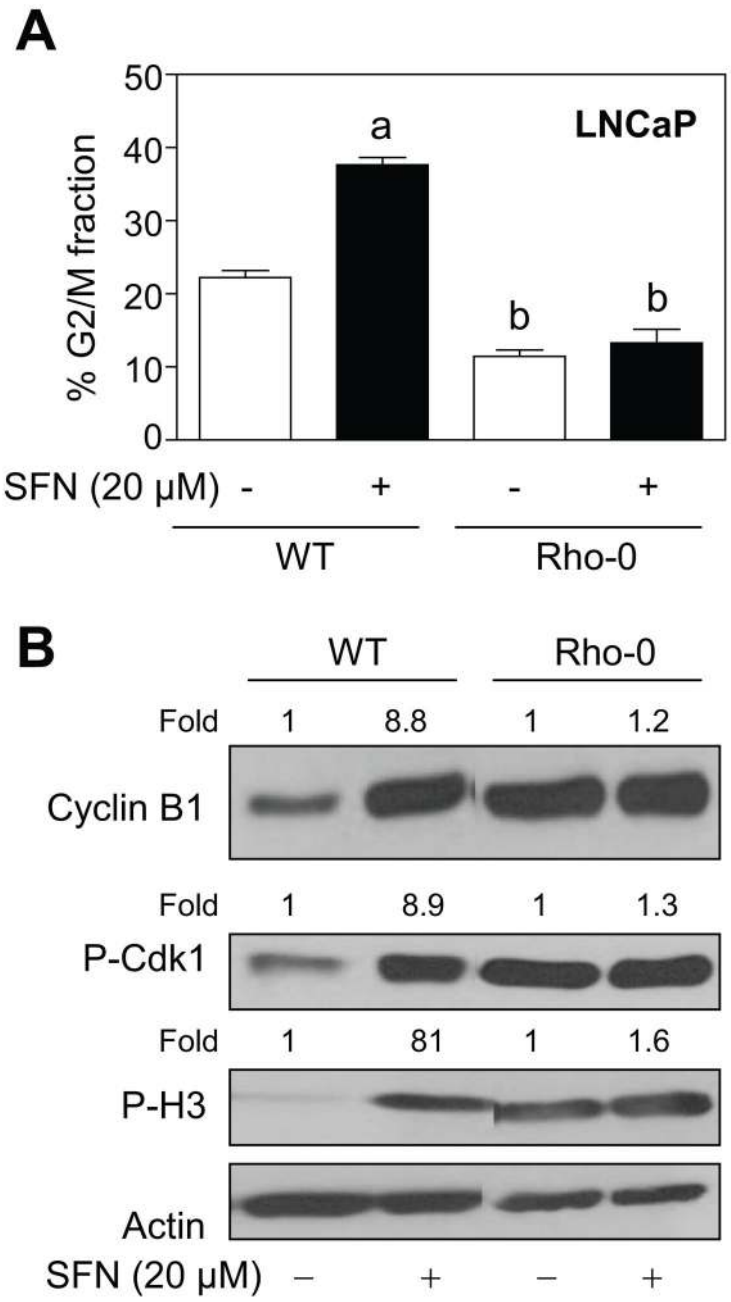

Fig. 4. SFN-induced G2/M arrest is dependent on mitochondria-derived ROS production

A,percentage of G2/M phase cells in wild-type LNCaP culture and its Rho-0 variant following 24 h treatment with DMSO or 20 μmol/L SFN. Results are mean ± SE (n= 3). Significantly different (P<0.05) compared with [a]corresponding DMSO-treated control and [b]SFN-treated wild-type cells by one-way ANOVA followed by Bonferroni's test. **B,** immunoblotting for cyclinB1, Tyr15 phosphorylated (inactive) cdk1, and Ser10 phosphorylated histone H3 (a marker of mitotic cells) using lysates from wild-type and Rho-0 PC-3 cells treated for 24 h with DMSO or 20 μmol/L SFN. The numbers on top of the immunoreactive bands represent change in protein levels relative to DMSO-treated control in both wild-type and Rho-0 PC-3

cells. Each experiment was performed at least twice and the results were comparable. Representative data from a single experiment are shown.

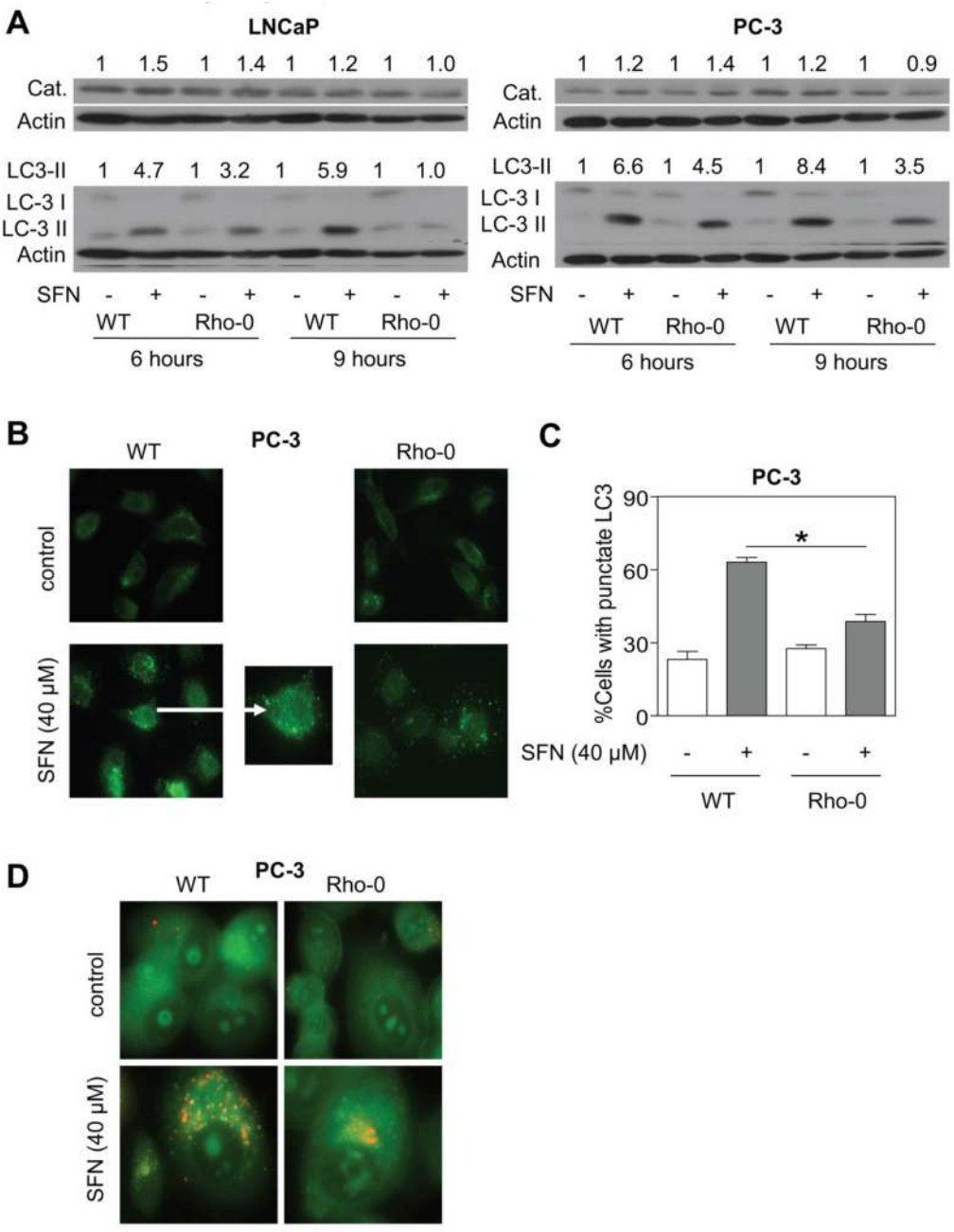

Fig. 5. SFN-induced autophagy in LNCaP and PC-3 cells is partially abrogated in Rho-0 cells

A,immunoblotting for catalase and cleaved LC3 (LC3-II) using lysates from wild-type LNCaP and PC-3 cells and their Rho-0 variants following 6 or 9 h treatment with DMSO or 40 μmol/L SFN. The numbers on top of the immunoreactive bands represent change in protein levels relative to DMSO-treated control in both wild-type and Rho-0 LNCaP and PC-3 cells. **B,** immunofluorescence analysis for punctate pattern of LC3 localization in wild-type PC-3 cells and its Rho-0 variant following 9 h treatment with DMSO or 40 μmol/L SFN (magnification 100×). **C,** percentage of cells with punctate pattern of LC3 localization in wild-type PC-3 culture and its Rho-0 variant following 9 h treatment with DMSO or 40 μmol/L SFN. Results are mean ± SE (n= 3). *Significantly different (P<0.05) between the indicated groups by one-way ANOVA followed by Bonferroni's test. **D,** visualization of acidic vesicular organelles

(yellow-orange) in wild-type PC-3 cells and its Rho-0 variant following 9 h treatment with DMSO or 40 μmol/L SFN (magnification 100×). Each experiment was performed at least twice and the results were comparable. Representative data from a single experiment are shown.

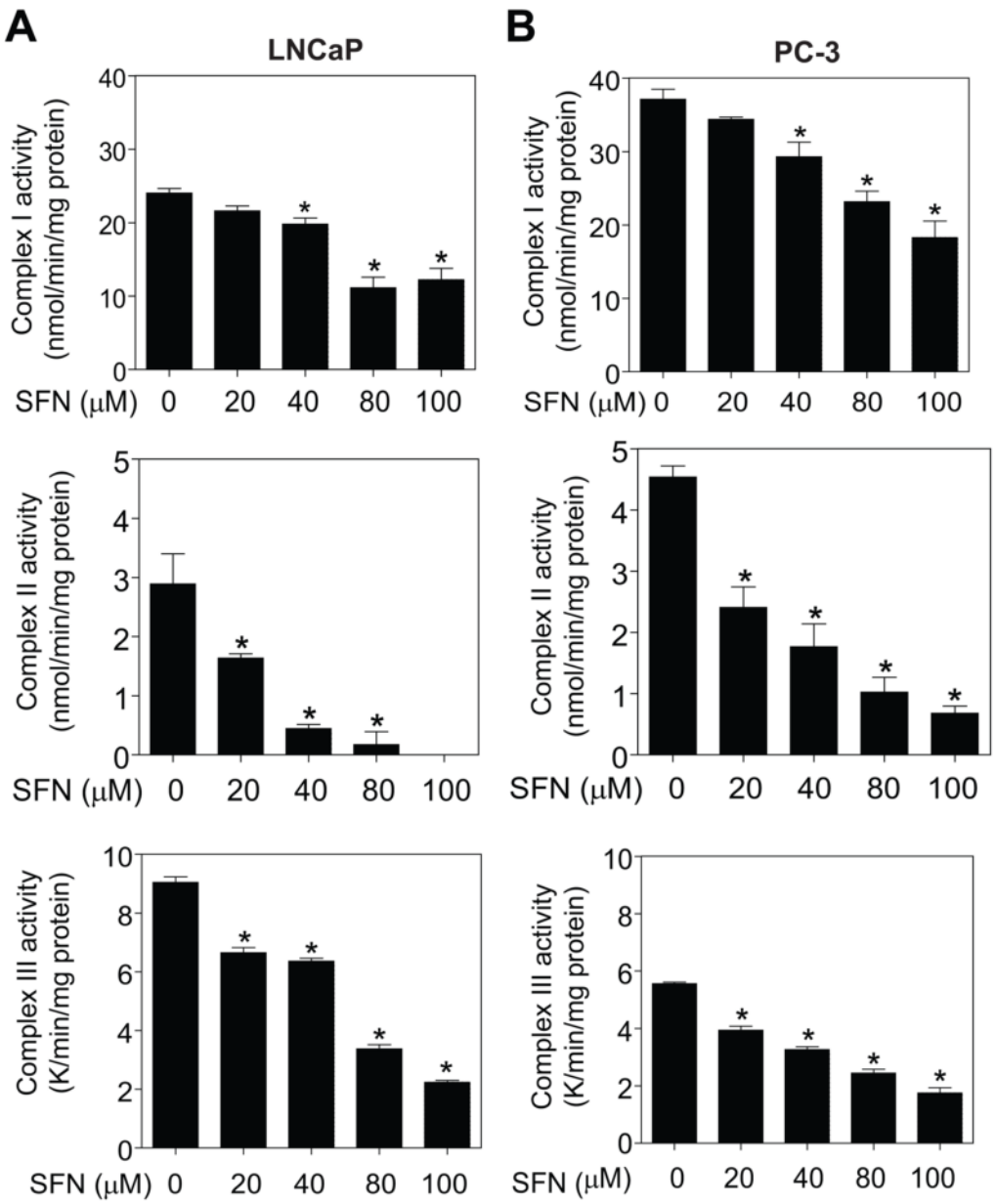

Fig. 6. SFN treatment inhibited MRC activities in LNCaP and PC-3 cells

Activities of complex I-linked NADH-ubiquinone oxidoreductase, complex II-linked succinate-ubiquinone oxidoreductase, and complex III-linked ubiquinol cytochrome *c* reductase in (A) LNCaP cells and (B) PC-3 cells treated for 6 h with DMSO (control) or the indicated concentrations of SFN. Results are mean ± SE (n= 3). *Significantly different (P<0.05) compared with control by one-way ANOVA followed by Dunnett's test. Each assay was performed at least twice using independently prepared cell extracts.